ELSEVIER

Journal of Chromatography A, 693 (1995) 113–130

JOURNAL OF CHROMATOGRAPHY A

Combined effects of non-linear electrophoresis and non-linear chromatography on concentration profiles in capillary electrophoresis

Michael S. Bello[1], Michael Yu. Zhukov[2], Pier Giorgio Righetti*

Faculty of Pharmacy and Department of Biomedical Sciences and Technologies, University of Milan, Via G. Celoria 2, 20133 Milan, Italy

First received 25 April 1994; revised manuscript received 26 July 1994; accepted 7 October 1994

Abstract

A theory of peak evolution in a column under the combined action of electromigration dispersion and equilibrium adsorption–desorption is presented. The basic equations for mass transport in zone electrophoresis are combined with those for non-linear chromatography. Langmuir's isotherm is assumed for describing the analyte interaction with the column wall (capillary electrophoresis in thin capillaries) or a sorbent (electrokinetic chromatography). The transport equation thus obtained is analysed and three specific cases determining the peak evolution are found: (A) the concentration velocity as a function of concentration is non-monotonous; (B) the velocity increases with analyte concentration; and (C) the velocity decreases with increments of concentration. Solutions to the transport equation for all three cases, describing the evolution of disperse boundary and discontinuities are derived. By assuming a "rectangular pulse" initial profile, a variety of peak shapes are generated. In the case of a non-monotonous velocity dependence on concentration, the initial concentration is shown to be an important parameter determining the peak shape and its transformations while moving along the column axis. A possibility of a counterbalance of the electromigration and adsorption mechanisms of the peak broadening, leading to a decay of the peak evolution into a "triangle" is found.

1. Introduction

Since the early 1980s [1], narrow-bore capillaries, down to 10 μm, have been used for electrophoretic separations. The main advantage of these capillaries is well known: they allow for significant decrease in the Joule heating and, thus, for an increase in the applied voltage leading to short separation times. Peak broadening mechanisms in these capillaries were found to be mostly the same as those in relatively wide capillaries (of about 2 mm I.D.) for which they were extensively studied many years ago [2,3].

Among others, these effects include electro-

* Corresponding author.

[1] Present address: Dionex Corp., 1228 Titan Way, Sunnyvale, CA 94088-3603 (USA).

[2] Permanent address: Department of Mechanics and Mathematics, Rostov State University, Zorge ul 5, Rostov-na-Donu 344104, Russian Federation.

0021-9673/95/$09.50
SSDI 0021-9673(94)00965-1

migration dispersion [4], i.e., an asymmetric peak broadening, caused by a mismatch between the electric conductivity of the analyte and the background electrolyte. The mass transport in electrophoresis is determined by the electric field. The presence of the analyte in the solution influences the electric conductivity of the solution and, therefore, the axial electric field in the column. This effect is expressed by a set of non-linear transport equations governing species concentrations in the solution.

It was understood by Virtanen [3] that interactions of an analyte with the capillary surface may affect the peak shape and electromigration time. However, these interactions were assumed to be negligible for large-bore capillaries. With narrow-bore capillaries, the analyte interactions with the capillary wall become important [5]. They even may be considered as one of the main obstacles to the progress of capillary electrophoresis (CE) and generated a great deal of research on surface coatings [6]. Such coatings should prevent analytes from being adsorbed on the wall, although it is doubtful that a universal coating that does not interact with all analytes exists.

The most elaborate method used to account for interactions of an analyte moving down a column with a solid phase is that developed in non-linear chromatography [7–9]. The transport equation governing analyte concentration in chromatography is derived by combination of the mass balance equation in the moving phase and the balance between solid and liquid phases. In the case of equilibrium between phases, the phase balance is described by Langmuir's isotherm, which leads to a non-linear transport equation.

This paper presents a novel theory uniting both mechanisms of peak broadening: electromigration dispersion and peak broadening due to adsorption. A brief review of electromigration and adsorption mechanisms of peak broadening is followed by derivation of the basic equation for the equilibrium mass transport in thin capillaries. Detailed analysis of this equation predicts various scenarios of the peak evolution.

2. Equations for zone electrophoresis and chromatography

This section presents known concepts from the theory of electrophoresis and non-linear chromatography.

2.1. Electrophoresis

Electrophoretic mass transport is modelled in a non-diffusion approximation by the following set of equations [10–12]:

$$\frac{\partial c}{\partial t} + \frac{\partial i_e}{\partial x} = 0 \tag{1}$$

$$i_e = \mu c E \tag{2}$$

$$\sigma = \sigma_0(1 + \alpha c), \quad j = \sigma E \tag{3}$$

where c is the concentration of an analyte, i_e is the electrophoretic mass flux, t is the time, x is the axial coordinate, μ is the electrophoretic mobility, E is the electric field strength, σ is the electric conductivity of the solution, σ_0 is the electric conductivity of the pure buffer, α is the concentration coefficient of the electric conductivity of the solution and j is the density of the electric current.

The dependence of the electric conductivity on the analyte concentration given by Eq. 3 is valid only for dilute solutions.

Excluding electric field strength from Eqs. 1–3, one finds

$$\frac{\partial c}{\partial t} + \frac{\partial}{\partial x}\left(\frac{\mu E_0 c}{1 + \alpha c}\right) = 0, \quad E_0 = \frac{j}{\sigma_0} \tag{4}$$

The solution for Eq. 4 with initial conditions in the form of a "rectangular pulse",

$$c(x,t)|_{t=0} = \begin{cases} c_0, & 0 \le x \le x_0 \\ 0, & x < 0, \quad x_0 < x \end{cases} \tag{5}$$

is well known [10,13]. It is shown in Fig. 1 (1.1 and 1.2) for positive and negative values of the parameter α.

For $\alpha > 0$ transformations of the initial profile are shown in Fig. 1 (1.1). The initial profile (A) evolves, after the motion starts, into the profile (B) with a rear discontinuity, having a coordi-

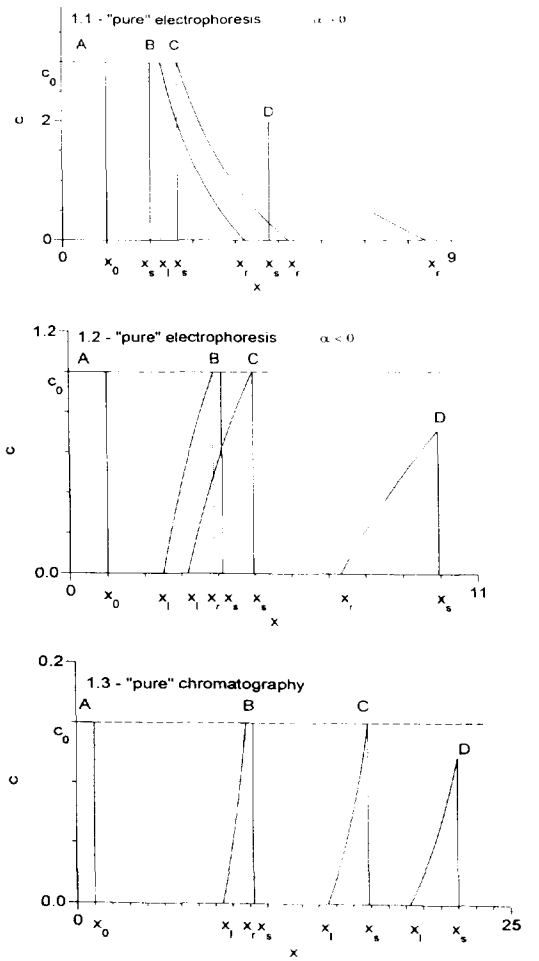

Fig. 1. Here and in all subsequent, relevant figures, patterns A–D represent the concentration profiles taken at different time moments along the column axis. The dashed vertical line is located at the point $x_l(t)$, called the left edge of the dispersed boundary, with which the rear discontinuity (vertical solid line) will merge at a certain time moment (here represented by profile C). In all relevant figures, x represents the column length. (1.1) Peak evolution in electrophoresis in the case $\alpha > 0$, $\alpha = 0.2$; (1.2) peak evolution in electrophoresis in the case $\alpha < 0$, $\alpha = -0.2$; (1.3) peak evolution in non-linear chromatography, $k_1 = 0.3$, $k_2 = 4$.

nate $x_s(t)$ at a time moment t, a region of the constant concentration and front disperse boundary. The front disperse boundary is bounded by a point $x_l(t)$ and a point $x_r(t)$ which we shall call the left edge and the right edge of the disperse boundary, respectively. The rear discontinuity moves faster than the left edge of the front disperse boundary and after a certain time catches it, eliminating the region of the constant concentration (C). After this moment the peak becomes "triangle"-like (D) with a rear discontinuity and a front disperse boundary. In the case of $\alpha < 0$ [Fig. 1 (1.2)], the initial profile (A) is subjected to similar transformations (B), (C) and (D). In both instances the peak evolution is characterized by the formation of a moving discontinuity, the coordinate of which is denoted by x_s, a disperse boundary with left edge x_l and right edge x_r.

Here a remark on the terminology is appropriate. The reader has probably realized that this paper deals with the phenomena called "non-linear waves", the mathematical theory of which was developed by Lax [14–16] and for electrophoresis [11]. Works on non-linear waves in chromatography have been recently reviewed by Helffrich [7] and Helffrich and Carr [8]. It was pointed out [7,8] that non-linear waves have been studied in mathematics, fixed-bed engineering and chromatography (we now add electrophoresis to this list) and it led to different terminologies used in different fields but describing the same phenomena. The most precise terminology has been developed in mathematics, but for chemists it might be rather unusual. We tried to find a compromise in this paper between rigorousness of definitions and intuition. The terminology used to describe the patterns shown in Fig. 1 (1.1 and 1.2) will be used in subsequent figures, where applicable. Therefore, we reserve the word *discontinuity* for what is also called "shock" or "abrupt transition" and denote its coordinate by x_s, $\bar{x}_s$ or $\bar{x}_s$. A region in space where the concentration monotonously increases or decreases is called a *disperse boundary*. It is bounded by its *left edge* x_l and the *right edge* x_r. A region where the substance concentration is not zero will be called a *peak* or *zone*. The region of the peak where the concentration increases along the space coordinate, even discontinuously, will be called the *peak rear* and

that where it decreases will be called the *peak front* (see [8]).

2.2. Non-linear chromatography

Non-linear, non-equilibrium chromatography of a single analyte is governed by the following set of equations [17,18]:

$$\frac{\partial c}{\partial t} + \frac{\partial i_c}{\partial x} + \frac{\partial q}{\partial t} = 0\,, \quad i_c = Vc \tag{6}$$

$$\frac{\partial q}{\partial t} = k_a(S - q)c - k_d q \tag{7}$$

where c is the concentration of the analyte in the liquid phase, i_c is the chromatographic mass flux, q is the analyte concentration in the immobile phase, V is the velocity of the liquid, k_a and k_d are coefficients of the adsorption and desorption, respectively, and S is the concentration of the binding sites in the immobile phase (we assume the porosity of the medium to be included in the coefficients k_a and k_d).

In the case of equilibrium chromatography, the concentration q in the immobile phase may be expressed through c. By neglecting fast processes in the establishment of the phase equilibrium, one can simplify Eqs. 6 and 7 to

$$\frac{\partial c}{\partial t} + \frac{\partial (Vc)}{\partial x} + \frac{\partial}{\partial t}\left(\frac{k_a S c}{k_a c + k_d}\right) = 0\,, \quad q = \frac{k_a S c}{k_a c + k_d} \tag{8}$$

The second expression for q in Eqs. 8 is known as the Langmuir isotherm.

The evolution of the "rectangular-pulse" initial profile predicted by Eqs. 8 is shown in Fig. 1 (1.3). The non-linear chromatographic peak evolution resembles that of zone electrophoresis when $\alpha < 0$ but the curvature of the rear disperse boundary is different.

In order to model mass transport in capillary zonal electrophoresis (CZE), we suggest combining the equation for the electrophoretic peak evolution (Eq. 4) with those of non-linear chromatography (Eqs. 8). These combined equations govern both the specific electrophoretic interaction of the sample with the buffer and mass exchange with the capillary wall, i.e., the immobile phase. These equations are also valid for electrokinetic chromatography [19,20].

3. Equations for zone electrophoresis in thin capillaries

The following combined equation is suggested for the modeling of the electrophoretic transport in thin capillaries where mass exchange with the capillary wall becomes significant:

$$\frac{\partial}{\partial t}\left(c + \frac{k_a S c}{k_a c + k_d}\right) + \frac{\partial}{\partial x}\left(Vc + \frac{\mu c E_0}{1 + \alpha c}\right) = 0 \tag{9}$$

where c is the analyte concentration in the buffer, k_a and k_d are the adsorption and desorption constants, respectively, μ is the electrophoretic mobility, E_0 is the electric field strength which would exist in the capillary in the absence of the sample and α is the concentration coefficient of the electric conductivity.

The term Vc in Eq. 9 describes, in particular, electroosmotic transport in the capillary. In this case the velocity V should be related to the electric field strength:

$$V = \mu_{os} E_{eff} \tag{10}$$

where μ_{os} is the effective electroosmotic mobility and E_{eff} is the effective electric field strength, proportional to the intensity of the external electric field. The effective electroosmotic mobility and the electric field strength may depend on the concentration of the analyte in the mobile and immobile phases, buffer pH, etc. As a rough approximation, they could be set at μ_{os} = constant and $E_{eff} = E_0$. In this paper we neglect effects of the electroosmotic transport and forced fluid flow, assuming

$$V = 0 \tag{11}$$

In order to transform Eq. 9 in a convenient form, the following dimensionless variables and characteristic values are introduced:

$$x = x' L_*\,, \quad t = t' \tau_*\,, \quad c = c' c_*\,,$$

$$k_1' = \frac{k_a}{k_d} \cdot S\,, \quad k_2' = \frac{k_a}{k_d} \cdot c_*\,, \tag{12}$$

$$\alpha' = \alpha c_*\,, \quad \tau_* = \frac{L_*}{\mu E_0}$$

where L_*, τ_*, c_* are the characteristic values (scales) of the length, time and concentration, respectively. Dimensionless variables and parameters in Eq. 12 are those primed. However, in order to make the following treatment more readable, we omit primes and assume all variables to be dimensionless.

A possible choice of the scales in Eq. 12 is the length of the capillary or the width of the initial peak x_0 as the length scale L_* and the buffer concentration as the concentration scale c_*.

Eq. 9 may be rewritten in the following form:

$$\frac{\partial \psi}{\partial t} + \frac{\partial \phi}{\partial x} = 0 \tag{13}$$

$$\psi = \psi(c) = c + \frac{k_1 c}{1 + k_2 c}, \quad \phi = \phi(c) = \frac{c}{1 + \alpha c} \tag{14}$$

where ϕ is the dimensionless density of the mass flux and ψ is the sum of the dimensionless concentrations in the liquid and immobile phases.

Evidently, Eq. 4 is a particular case of Eqs. 13 and 14 describing "pure" electrophoresis when $k_1 = 0$ (and $k_2 = 0$). Eqs. 8 for "pure" chromatography are another particular case of the same equations at $\alpha = 0$ (formally, in this case $V = 1$).

Eqs. 13 and 14 and also Eqs. 4 and 8 are not applicable to discontinuities. Solutions of these equations represent only disperse boundaries or regions of constant concentration. However, the usual approach is to study the evolution of the initial peak in the form of a "rectangular pulse", i.e., a discontinuous profile (see Fig. 1). In this case Eq. 13 should be supplemented with a condition relating fluxes and concentrations at both sides of the discontinuity:

$$D_{c_l, c_r}\{\psi(c_l) - \psi(c_r)\} = \phi(c_l) - \phi(c_r),$$

$$\frac{dx_s(t)}{dt} = D_{c_l, c_r} \tag{15}$$

where c_l and c_r are the concentrations at a close vicinity to the left and right sides of the discontinuity, respectively; D_{c_l, c_r} denotes the velocity of the discontinuity motion along the capillary and $x_s(t)$ is the axial coordinate of the discontinuity. We shall also use another notation for the velocity of the discontinuity: $D\{c_l, c_r\}$ explicitly showing its functional dependence on c_l and c_r (see [14–16]).

An explanation to Eq. 15 is the following. Assume that at the left side of the discontinuity the analyte concentration in the mobile and immobile phases is $\psi = \psi(c_l)$ and the flux density is $\phi = \phi(c_l)$. At the right side of the discontinuity $\psi = \psi(c_r)$ and $\phi = \phi(c_r)$. The mass flux due to the motion of the discontinuity is equal to $D_{c_l, c_r}\{\psi(c_r) - \psi(c_l)\}$. According to the law of mass conservation it should be balanced by the difference of the fluxes $\phi(c_r) - \phi(c_l)$ as it is expressed by Eq. 15.

Eqs. 13 and 14 are subjected to the following physical constraints: concentration c is positive or zero, coefficients k_1 and k_2 are positive or zero (see Eqs. 16) and electric conductivity is positive (see Eq. 17):

$$c(x, t) \geq 0, \quad k_1 \geq 0, \quad k_2 \geq 0 \tag{16}$$

$$1 + \alpha c(x, t) > 0 \tag{17}$$

The concentration coefficient of conductivity α is supposed to have both signs and, in particular, to be zero.

The initial conditions for Eqs. 13–17 are Eq. 5.

The set of equations Eqs. 13–17 and 5 represents the simplest non-linear mathematical model taking into account effects of the electrodispersion and interaction with the capillary wall (or the sorbent, in electrokinetic chromatography). Solutions to this kind of equations are known to exhibit "non-uniqueness", i.e., they can give several values of concentration for one space point. In order to have a physically meaningful solution, additional conditions, further specified, should be added to Eqs. 13–17 and 5.

4. Dependence of velocity on concentration

The concentration dependence of the concentration velocity is of decisive importance for a peak profile. This section studies possible dependences of the concentration velocity on con-

centration and relates them to the shape of the peak.

Eqn. 13 may be represented in the form

$$\frac{d\psi}{dc}\cdot\frac{\partial c}{\partial t}+\frac{d\phi}{dc}\cdot\frac{\partial c}{\partial x}=0$$

which transforms to the well known transport equations for concentration c [8,11,14–16]:

$$\frac{\partial c}{\partial t}+v(c)\frac{\partial c}{\partial x}=0 \qquad (18)$$

where $v(c)$ is the concentration velocity. By comparing Eq. 18 with the previous one, we derive

$$v(c)=\frac{\phi'(c)}{\psi'(c)} \qquad (19)$$

Taking into account Eq. 14 one obtains an explicit expression for $v(c)$:

$$v(c)=\frac{1}{(1+\alpha c)^2}\cdot\frac{(1+k_2c)^2}{k_1+(1+k_2c)^2} \qquad (20)$$

Analysing the dependence of the concentration velocity $v(c)$ on the parameters k_1, k_2 and α, one can distinguish three cases: (i) the velocity is non-monotonous (Fig. 2A-i); (ii) the velocity increases with increasing concentration (Fig. 2A-ii); (iii) the velocity decreases with an increase in concentration (Fig. 2A-iii). The following relationships determine the three cases:

$$\text{(i)}\quad k_1(k_2-\alpha)>\alpha\,,\quad \alpha>0 \qquad (21)$$

$$\text{(ii)}\quad \alpha<0\,,\quad (1+\alpha c)>0 \qquad (22)$$

$$\text{(iii)}\quad k_1(k_2-\alpha)<\alpha\,,\quad \alpha>0 \qquad (23)$$

The maximum velocity v_m and the concentration c_m corresponding to it in Fig. 2A-i are given by

$$c_m=\frac{1}{k_2}\left\{\left[\frac{k_1(k_2-\alpha)}{\alpha}\right]^{1/3}-1\right\},$$

$$v_m=\max_{c\geq 0}v(c)=v(c_m) \qquad (24)$$

Let us consider the evolution of the initial peak rear. The initial distribution of the concentration is given by Eq. 5. At the initial moment the analyte concentration c at $x=0$ lies within the range $0\leq c\leq c_0$.

When the electric field is applied, each point on the analyte moves with the velocity given by Eq. 20 (Figs. 2A-i, 2A-ii and 2A-iii) and in the time moment close to $t=+0$, transforms to the shapes shown in Figs. 2B-i, 2B-ii and 2B-iii. The arrows in Figs. 2B indicate the velocities of the points having different concentrations. The graphs in Figs. 2B were obtained from those in Figs. 2A by a reflection relative to the bisector of the coordinate angle. Figs. 2B illustrate that for a peak rear the points of the initial concentration profile move according to

$x=v(c)t$ or, in another form,

$$v(c)=z\,,\quad z=\frac{x}{t} \qquad (25)$$

For a peak front the points of the initial concentration profile move according to

$x=x_0+v(c)t$ or, in another form,

$$v(c)=z\,,\quad z=\frac{x-x_0}{t} \qquad (26)$$

where z is the variable proportional to the coordinate x at any time moment t.

Eq. 25 determines in an implicit fashion a dependence of the analyte concentration on x and t.

Unfortunately, an explicit equation for $c(z)$ is difficult to obtain. However, for a qualitative analysis, the explicit equation is not necessary. In fact, the function $c(z)$ is already shown in Figs. 2B.

Not all of the peaks shown in Figs. 2B may exist. Thus, at a time moment t_1 there are three different values of concentration corresponding to one space point $x_1=z_1t_1$ in Fig. 2B-i and two different concentration values in Fig. 2B-iii (see the vertical dashed lines). This situation, obviously, cannot exist. Only in Fig. 2B-ii does the transformed profile have the necessary property of uniqueness and, thus, is compatible with real experimental conditions. In order to avoid non-uniqueness of the profiles shown in Figs. 2B-i and 2B-iii, a discontinuous profile should be realized. Its motion is determined by Eq. 15. Additionally, only one of the two branches of the profile in Fig. 2B-i can exist. A solution to

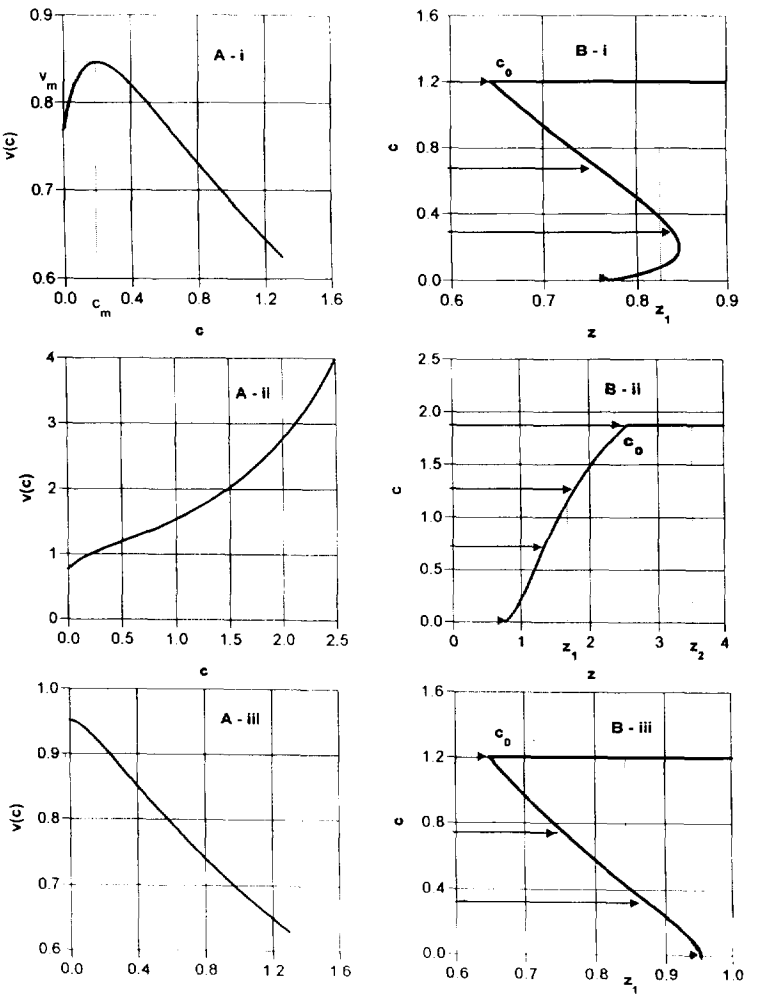

Fig. 2. Dependence of the concentration velocity on the concentration (A) and a transformation of the edges of the initial "rectangular pulse" (B). (A-i, B-i) Non-monotonous dependence of the concentration velocity on the concentration. $k_1(k_2-\alpha)>\alpha$, $\alpha=0.2>0$, $k_1=0.3$, $k_2=4$, $c_0=1.2$. (A-ii, B-ii) Monotonously increasing dependence of the concentration velocity on the concentration. $1+\alpha c>0$, $\alpha=-0.2<0$, $k_1=0.3$, $k_2=4$, $c_0=1.8$. (A-iii, B-iii) Monotonously decreasing dependence of the concentration velocity on the concentration. $k_1(k_2-\alpha)<\alpha$, $\alpha=0.2>0$, $k_1=0.05$, $k_2=4$, $c_0=1.2$.

Eq. 25 or 26 for case (i), corresponding to Fig. 2B-i, can be represented in the following form:

$$c(z)=\begin{cases}c_1(z), & \text{for } 0\leq c\leq c_m, \quad z=v(c_1)\\ c_2(z), & \text{for } c_m<c\leq c_0, \quad z=v(c_2)\end{cases} \tag{27}$$

where $c_1(z)$ and $c_2(z)$ are two branches of the inverse function $c=v^{-1}(z)$.

The requirement of the uniqueness of the concentration at any space point makes impossible the existence of disperse boundaries in Fig. 2B-ii and for $0\leq c\leq c_m$ (Fig. 2B-i) at the peak front. Analogously, the existence of the disperse boundary in Fig. 2B-iii and for $c_m\leq c\leq c_0$ 2B-i at the peak rear is impossible.

Fig. 3 illustrates an evolution of the whole initial peak in case (i), Eq. 21, when the concentration velocity is non-monotonous. Lines (a, b) and (c, d) show the lines of discontinuities in the profile. Evidently, the upper branch of the profile should be rejected at the rear and the lower branch should be rejected at the front of

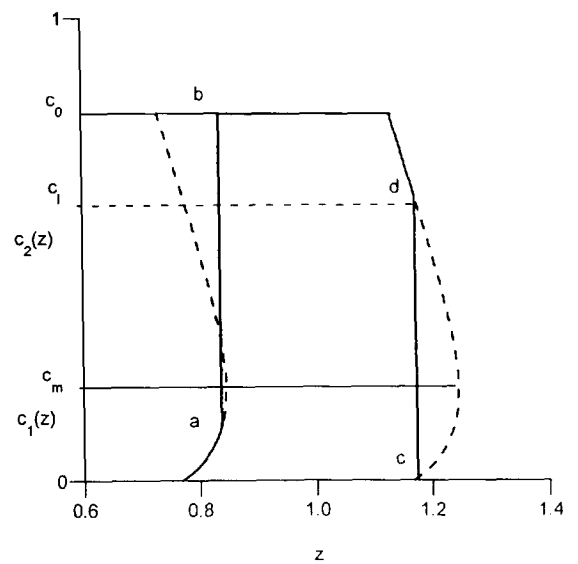

Fig. 3. Scheme of the "rectangular pulse" transformation when the concentration velocity is not monotonous. c_m is the concentration corresponding to the maximum velocity; a, b and c, d are the lines of discontinuities imposed to obtain uniqueness of the concentration. Dashed curves indicate non-existent solutions.

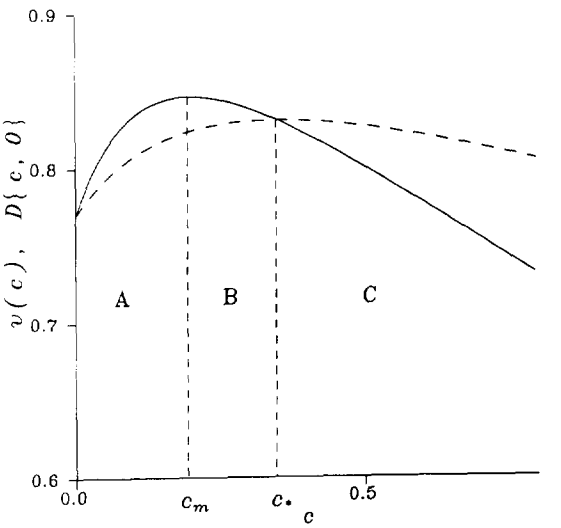

Fig. 4. Dependence of the concentration velocity $v(c)$ (solid curve) and the velocity of the discontinuity $D\{c,0\}$ (dashed curve) on concentration. $\alpha = 0.2$, $k_1 = 0.3$, $k_2 = 4$.

the peak (dashed lines). These two dashed lines would again violate the principle of concentration uniqueness at some given space points and, thus, have to be rejected. Locations of the discontinuities are regulated by Eq. 15.

It may occur that a discontinuity is not stable, i.e. it also cannot exist. Thus, consider a discontinuity at the peak front, line (c, d) in Fig. 3. The concentration at the left side of the discontinuity is c_l and at the right side $c_r = 0$. As $\psi(0) = 0$ and $\phi(0) = 0$ (see Eq. 14), the velocity of the discontinuity found according to Eq. 15 is

$$D_{c_l,0} = \frac{\phi(c_l)}{\psi(c_l)} = \frac{1 + k_2 c_l}{(1 + k_1 + k_2 c_l)(1 + \alpha c_l)} \qquad (28)$$

Fig. 4 shows the dependence of the discontinuity velocity $D_{c,0}$ on the concentration c. The concentration velocity $v(c)$ is shown by a dashed line. The two curves have an intersection point at concentration c_*, i.e.,

$$v(c_*) = D_{c_*,0} = D\{c_*, 0\}$$

$$c_* = \frac{1}{k_2}\{(1 + k_2 c_m)^{3/2} - 1\}$$

$$= \frac{1}{k_2}\left\{\left[\frac{k_1(k_2 - \alpha)}{\alpha}\right]^{1/2} - 1\right\} > c_m \qquad (29)$$

It is seen from Fig. 4 that

$$v(c) \geq D_{c,0}, \quad 0 \leq c \leq c_* \qquad (30)$$

$$v(c) \leq D_{c,0}, \quad c_* \leq c \leq c_0 \qquad (31)$$

When the concentration velocity is less than the velocity of the discontinuity, Eq. 31, the discontinuity cannot exist, as the concentration at the left side of the discontinuity lags behind it and thus destroys the discontinuity. In contrast, in the case given by Eq. 30, the concentration at the left side of the discontinuity moves faster than the discontinuity. This leads to non-uniqueness of the concentration profile and, thus, to the necessity for the discontinuity.

In particular, for $c_0 \geq c_*$, the discontinuous profile of the left edge shown in Fig. 3 exists only if $c_l \geq c_*$.

A general condition of the discontinuity stability is given by

$$v(c_l) \geq D_{c_l,c_r} \geq v(c_r) \tag{32}$$

A concentration profile giving a solution to the problem in Eqs. 13–17 is found by combining solutions of Eq. 27 and introducing discontinuities where the solutions of Eq. 27 are not unique. The discontinuities should satisfy Eqs. 15 and 32. All stages of the peak evolution for the cases (i)–(iii) (as illustrated in Figs. 2) are described in the following section.

5. Peak evolution

This section deals with evolutions of the initial profile for the three types of the velocity dependence on the concentration (Eqs. 21–23).

The most interesting case, generating a variety of peak shapes, is when the dependence of the velocity on concentration has a maximum. A condition for the existence of the maximum is given by Eq. 21.

5.1. Case (i). Peak evolution with non-monotonous velocity; $k_1(k_2 - \alpha) > \alpha$, $\alpha > 0$

The concentration c_m, corresponding to the maximum of the concentration velocity, and the concentration c_*, corresponding to the equality of the concentration velocity to the velocity of the discontinuity, divide the whole range of the initial concentration c_0 into three intervals (see Fig. 4):

(A) $c_0 < c_m$, the interval of low initial concentration;

(B) $c_m < c_0 < c_*$, the interval of intermediate initial concentration;

(C) $c_* < c_0$, the interval of high initial concentration.

The behaviour of the concentration profile depends on the interval to which the initial concentration belongs. It is analysed successively below for all three intervals.

(A) Interval of low initial concentration, $c_0 < c_m$ (see Fig. 4)

Under the condition in which the initial concentration is less than the concentration c_m corresponding to the maximum of $v(c)$, only the first branch of the function $c = c_1(z)$ exists, Eq. 27. Successive stages of the initial profile evolution are shown in Figs. 5 and 6. Fig. 5 presents patterns at different time moments as they move along the capillary axis in the same length scale. The structure of the peaks is shown on a larger scale in Fig. 6. At the time moment $t = +0$ the initial profile (Fig. 6A) transforms into the peak shown in Fig. 6B. The left edge of the rear disperse boundary x_l moves along the x-axis with constant velocity $v(0)$:

$$x_l(t) = v(0)t \tag{33}$$

The concentration in the rear disperse boundary between x_l and x_r is given by the function $c_1(z)$, Eq. 27. The right edge of the rear disperse boundary $x_r(t)$ also moves with constant velocity $v(c_0)$:

$$x_r(t) = v(c_0)t \tag{34}$$

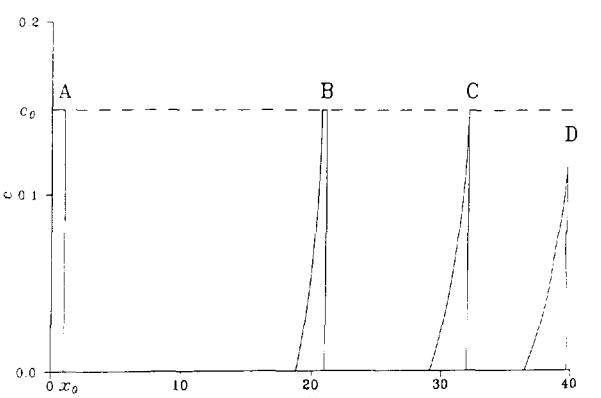

Fig. 5. Peak evolution for non-monotonous velocity and low initial concentration $c_0 < c_m$. (A), (B), (C) and (D) are the peak shapes at dimensionless time moments $t = 0$, 24.5, 36.45 and 38.3, respectively. Parameters: $\alpha = 0.2$, $k_1 = 0.3$, $k_2 = 4$, $c_0 = 0.15$. Values of $c_m = 0.1966$ and $c_* = 0.3470$. $v(0) = 0.7692$, $v(c_0) = 0.8437$, $D_{c_0,0} = 0.8176$.

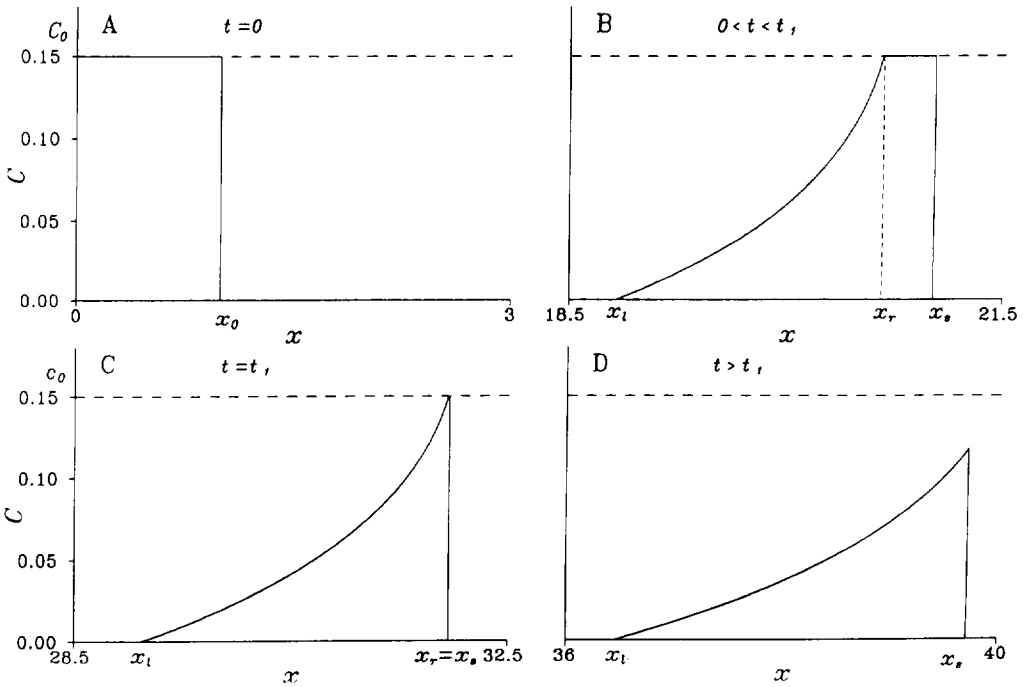

Fig. 6. Structure of the peaks shown in Fig. 5. Peaks A and B are plotted in the same scale (on the x-axis), which is, however, different from the scale used for peaks C and D. (A) Initial "rectangular pulse" distribution at $t = 0$, $x_0 = 1$. (B) A peak with a developed disperse rear boundary, a region of constant initial concentration and a sharp discontinuity at the front. (C) A peak at the time moment $t = t_1 = 38.3$ when the disperse boundary reaches the front. The concentration of the peak maximum is still the initial concentration. (D) A "triangle"-like peak at $t = 47.4$. Note that, in this last instance, the peak maximum has decreased.

As the velocity corresponding to the initial concentration c_0 is higher than the velocity corresponding to the zero concentration $v(c_0) > v(0)$, the width of the rear disperse boundary $x_r - x_l = \{v(c_0) - v(0)\}t$ increases linearly with time. The peak front is a sharp discontinuity which moves along the x-axis with constant velocity $D_{c_0,0}$:

$$x_s(t) = x_0 + D_{c_0,0}t \tag{35}$$

It is seen from Fig. 4 that the stability condition of the discontinuity, Eq. 32, is satisfied, i.e., $v(c_0) > D_{c_0,0} > v(0)$. It follows from this inequality that the edge $x_r(t)$ will catch up the front discontinuity $x_s(t)$ at the time moment t_1 (Fig. 6C):

$$x_r(t_1) = x_s(t_1), \quad t_1 = \frac{x_0}{v(c_0) - D_{c_0,0}} \tag{36}$$

Further development of the peak is determined by the velocity of the discontinuous front, Eq. 28, which is not algebraic in this case, but an ordinary differential equation:

$$\frac{d\bar{x}_s(t)}{dt} = D\{c_1, 0\} = \frac{1 + k_2 c_1(\bar{x}_s/t)}{[1 + k_1 + k_2 c_1(\bar{x}_s/t)][1 + \alpha c_1(\bar{x}_s/t)]} \tag{37}$$

with the initial condition

$$\bar{x}_s(t_1) = x_s(t_1) = x_r(t_1) = \frac{v(c_0)x_0}{v(c_0) - D_{c_0,0}} \tag{38}$$

where $\bar{x}_s(t)$ is a new function describing a position of the peak front after the time t_1 given by Eq. 36.

A general case, like the Gauche problem in Eqs. 37 and 38, can be solved only by computer

methods. However, the peak behaviour in the final stage can be easily analysed in an asymptotic form.

The final stage of the peak evolution is shown in Fig. 6D. A "triangle"-like peak moves along the x-axis, keeping its shape. The concentration in the peak maximum decreases with time.

Asymptotic solution. Let us assume that after a relatively long time the concentration becomes small and later verify that. In this case it is easy to find an asymptotic solution to the problem in Eqs. 37 and 38. By expanding functions $\psi(c)$, $v(c)$ and $D_{c,0}$ (Eqs. 14, 20 and 28) in power series of c, and neglecting terms proportional to powers of c higher than two, one derives

$$\psi(c) \approx (1 + k_1)c\,, \quad v(c) \approx v(0) + v_c'(0)c\,,$$

$$D_{c,0} \approx v(0) + \frac{1}{2} v_c'(0)c$$

Then, it follows from Eq. 25 that

$$c_1(z) = \frac{z - v(0)}{v_c'(0)}\,, \quad z = \frac{x(t)}{t}\,, \quad x_1(t) \leq x \leq \bar{x}_s(t) \tag{39}$$

Eq. 37 simplifies to

$$\frac{d\bar{x}_s(t)}{dt} \approx \frac{1}{2}\left[\frac{\bar{x}_s(t)}{t} + v(0)\right] \tag{40}$$

A solution to Eq. 40 is given by

$$\bar{x}_s(t) = v(0)t + b\sqrt{(t)} \tag{41}$$

where b is the integration constant.

Constant b cannot be found from the initial condition, Eq. 38, as this equation does not assume small concentration values. For this purpose, the mass concentration law is applied. As ψ is the mass concentration in the mobile and immobile phases, the mass conservation law implies that

$$\int_{x_1(t)}^{\bar{x}_s(t)} \psi[c_1(y/t)]\,dy = m_0\,, \quad m_0 = x_0\psi(c_0)$$

where m_0 is the mass of the substance introduced in the column. By evaluating the integral with the approximated expression for $\psi(c)$, the following expression is found:

$$m_0 \approx \frac{1 + k_1}{2v'(0)} \cdot b^2$$

and, finally, the constant b is found as

$$b = \sqrt{\frac{2\psi(c_0)v'(0)x_0}{1 + k_1}} > 0 \tag{42}$$

The concentration at the point of discontinuity, which is the maximum concentration of the peak in this instance, is given by

$$c_s = c_1[\bar{x}_s(t)/t] \approx \frac{b}{v'(0)\sqrt{(t)}} \tag{43}$$

where c_s is the concentration at the discontinuity point.

The width of the peak Δx is given by

$$\Delta x(t) = \bar{x}_s(t) - x_1(t) = b\sqrt{(t)} \tag{44}$$

Therefore, the peak width increases with time proportionally to the square root of time. This is the same law that governs the peak width of a Gaussian peak, but the mechanism of the broadening and the peak shape are different. In contrast to a Gaussian peak, the peak we analyse here is asymmetric and its concentration grows linearly from zero at $x = x_1$, Eq. 33, to c_s at the point $x = \bar{x}_s$, given by Eqs. 41 and 43. The value of the function ψ at the discontinuity point is $\psi(c_s)$ and the total mass of the substance in the column may be found as the area of the triangle

$$m_0 = \frac{1}{2}\Delta x\,\psi(c_s) \tag{45}$$

Of course, Δx and c_s, as given by Eqs. 43 and 44, satisfy Eq. 45. The latter can be used as a simple way to determine the constant b.

Concluding the analysis of the peak evolution in the case of low initial concentration, the following scenario can be presented. At the initial stage of the peak evolution the left and right edges of the rear disperse boundary and the front discontinuity move with constant but different velocities (Fig. 6B). The velocity of the discontinuity is less than the velocity of the right edge of the rear disperse boundary (see Fig. 4).

After the time moment $t = t_1$, when the peak transformation occurs, i.e., when the disperse boundary reaches the front discontinuity (Fig. 6C), the velocity of the front decreases approaching the velocity of the left edge of the rear disperse boundary (Fig. 6D).

(B) Interval of intermediate initial concentration, $c_m < c_0 < c_*$ (see Fig. 4)

A specific feature of this interval of the initial concentration is that both branches $c_1(z)$ and $c_2(z)$ could exist (see Fig. 3 and Eq. 27). However, the branch $c_2(z)$, as was discussed above (Eqs. 30–32), exists only for initial concentrations higher than c_*.

The peak rear for the case in which the initial concentration c_0 is higher than the concentration c_m cannot be represented by a disperse boundary given by $c_1(z)$ and continuously matching the region of the constant initial concentration, as we have seen in the previous subcase of low initial concentration [the branch $c_1(z)$ exists only for $c < c_m$, Eq. 27]. However, it is possible to combine a solution $c_1(z)$ with a discontinuity (Fig. 3). The front of the peak can be represented as a discontinuity, since $c_0 < c_*$, and, therefore, the concentration velocity is higher than the velocity of the discontinuity (Fig. 4). The latter is required by Eq. 32.

Successive stages of the peak evolution are shown in Figs. 7 and 8. Fig. 7 presents all patterns in the same scale, whereas in Fig. 8 they are shown on an enlarged scale in order to describe their peculiarities. The initial rectangular profile (Figs. 7A and 8A) transforms at the time moment $t = +0$ into the peaks shown in Figs. 7B and 8B. The edges $x_1(t)$ and $x_s(t)$ move along the x-axis with the constant velocities $v(0)$ and $D_{c_0,0}$, respectively:

$$x_1(t) = v(0)t \tag{46}$$

$$x_s(t) = x_0 + D_{c_0,0}t \tag{47}$$

It is slightly more complex to determine the velocity and law of motion of the right edge of the rear disperse boundary. In order to find this velocity, Eq. 37 should be used. It has the following form in the present case:

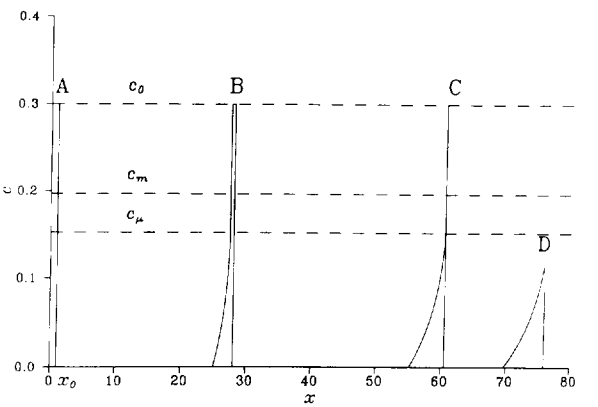

Fig. 7. Peak evolution for non-monotonous velocity and intermediate initial concentration $c_m < c_0 < c_*$. (A), (B), (C) and (D) are the peak shapes at dimensionless time moments $t = 0$, 32.62, 72.41 and 90.6, respectively. Parameters: α, k_1 and k_2 as in Figs. 5 and 6. $c_0 = 0.3$. Values of c_m, c_* and $v(0)$ as in Figs. 5 and 6. $\mu = 0.844$, $D_{c_0,0} = 0.83$, $c_1(\mu) = 0.152$.

$$\frac{dx_r}{dt} = D\{c_1(x_r/t), c_0\} \tag{48}$$

with the initial condition

$$x_r(0) = 0 \tag{49}$$

The value of $x_r(t)/t$ is indeterminate at $t = 0$. By using the L'Hospital rule for revealing indeterminacy, one finds

$$\lim_{t\to 0} \frac{x_r}{t} = \left.\frac{dx_r(t)}{dt}\right|_{t=0} = v_r(0) \equiv \mu_1$$

where μ_1 denotes the velocity of the right edge $v_r(0)$, still unknown at the initial time moment $t = 0$.

Eq. 48 at time $t = 0$ may be represented as follows:

$$\mu_1 = D\{c_1(\mu_1), c_0\} \tag{50}$$

Eq. 50 allows one to determine the velocity μ_1. We can easily solve it by noting that the velocity μ_1 is at the same time the concentration velocity, corresponding to a certain concentration c_{μ_1}, and the velocity of the discontinuity, having a concentration c_{μ_1} at the left and a concentration c_0 at the right. In order to find an approximate value of c_{μ_1}, one plots two functions, $y = D\{c, c_0\}$ and $y = v(c)$, and finds the

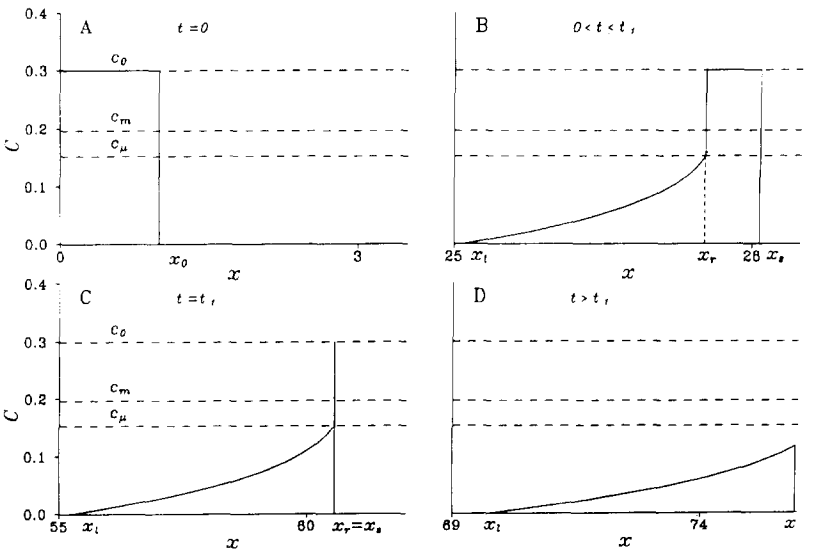

Fig. 8. Structure of the peaks shown in Fig. 7. Peaks A and B are plotted on the same scale (on the x-axis), which is, however, different from the scale used for peaks C and D. (A) Initial "rectangular pulse" distribution at $t = 0$, $x_0 = 1$. (B) A peak with a developed disperse rear boundary, right discontinuity, a region of constant initial concentration and a front discontinuity, $t = 32.62$. (C) A peak at the time moment $t = t_1 = 72.41$ when the disperse boundary reaches the front. The concentration of the peak maximum is still the initial concentration. (D) A "triangle"-like peak at $t = 90.6$.

point of their intersection having coordinates (c_{μ_1}, μ_1) (Fig. 9).

The solution to Eq. 48 is found in the following simple form:

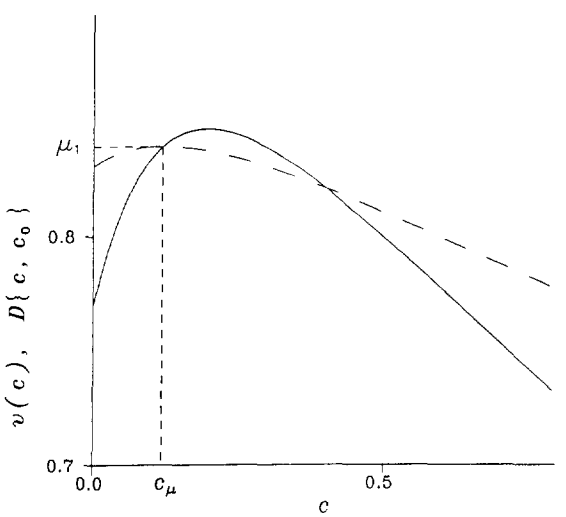

Fig. 9. Dependences of the concentration velocity and the velocity of the discontinuity D_{c,c_0} on concentration for $\alpha = 0.2$, $k_1 = 0.3$, $k_2 = 4$ and $c_0 = 0.4$.

$$x_r(t) = \mu_1 t \tag{51}$$

In order to verify this, it is sufficient to note that substituting $x_r(t)$ from Eq. 51 into Eq. 48 transforms the latter into an equation like Eq. 50 and the initial condition, Eq. 49, is also satisfied. It follows from Eq. 51 that the right edge of the disperse boundary x_r moves along the x-axis with a constant velocity μ_1. Concentration $c_1(\mu_1)$, corresponding to the concentration at the right edge of the rear disperse boundary, is the peak tail height. It is worth noting that this concentration is a constant until the time moment t_1 when the rear discontinuity reaches the front discontinuity.

At the time moment t_1, determined from the condition $x_r(t_1) = x_s(t_1)$, the right edge of the disperse boundary reaches the sharp front $x_s(t)$ (Figs. 7C and 8C). After this moment the peak shape becomes "triangle"-like (Figs. 7D and 8D), and the peak evolves analogously to the case considered above (Eqs. 41 and 43).

Summarizing the analysis presented above, the following scenario of the peak evolution in the

case of an intermediate initial concentration might be suggested. Similarly to the previous case of low initial concentration, the rear disperse boundary, the width of which grows linearly with time, and the discontinuity at the front are formed. However, another discontinuity at the right edge of the rear disperse boundary distinguishes this case from the previous one (compare Figs. 6B and 8B). A very interesting characteristic of the peak evolution shown in Figs. 7 and 8 is that the peak height falls abruptly from c_0 to c_{μ_1} at $t = t_1$. It is also worth noting that the time moment t_1 when the rear disperse boundary reaches the front and the location of this event at the x-axis are almost twice as long in comparison with the case of low concentration. This means that one observes either a triangle or a peak having a rectangular region depending on the initial concentration of the analyte.

(C) Interval of high initial concentration, $c_m < c_* < c_0$ (see Fig. 4)

The initial peak transformations are shown in Figs. 10 and 11. The development of the rear disperse boundary combined with the discontinuity is essentially the same as in the previous case. However, the front region of the peak cannot be represented as a pure discontinuity as

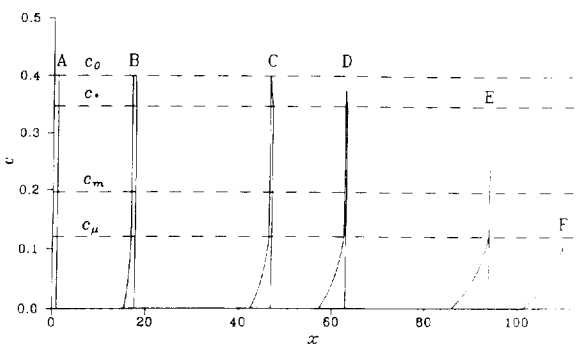

Fig. 10. Peak evolution for the non-monotonous velocity and high initial concentration $c_m < c_* < c_0$. (A), (B), (C), (D), (E) and (F) are the peak shapes at dimensionless time moments $t = 0$, 20.1, 55.3, 74.5, 111.5 and 131.5, respectively. Parameters α, k_1 and k_2 and the values of c_m, c_* and $v(0)$ as in Figs. 5–8. $c_0 = 0.4$, $\mu_1 = 0.839$, $c_1(\mu_1) = 0.12$, $\mu_2 = 0.831$, $c_2(\mu_2) = c_*$.

the stability condition for the discontinuity is not satisfied there (the velocity of the discontinuity is higher than the concentration velocity at the left from the discontinuity, see Fig. 4, $c > c_*$). Therefore, the concentration profile at the front boundary of the peak should be a combination of the profile $c_2(z)$ and a discontinuity, in analogy with that found in the previous case for the rear disperse boundary.

The right and left edges of the rear disperse boundary move along the x-axis with constant velocities:

$$x_l(t) = v(0)t\,, \quad x_r(t) = \mu_1 t \tag{52}$$

where μ_1 is the velocity found from Eq. 50.

The motion of the left edge of the front disperse boundary is governed by

$$\bar{x}_l(t) = v(c_0)t + x_0 \tag{53}$$

where $\bar{x}_l(t)$ is the coordinate of the left edge of the front disperse boundary.

The equations for the right edge of the front disperse boundary will then be similar to Eqs. 48 and 49:

$$\frac{d\bar{x}_r}{dt} = D\left\{c_2\left(\frac{\bar{x}_r - x_0}{t}\right), 0\right\} \tag{54}$$

$$\bar{x}_r(0) = x_0 \tag{55}$$

Again, as in the previous case of intermediate initial concentration,

$$\lim_{t\to 0}\frac{\bar{x}_r - x_0}{t} = \left.\frac{d(\bar{x}_r(t) - x_0)}{dt}\right|_{t=0} \equiv \mu_2 \tag{56}$$

where μ_2 is the velocity of the right edge of the front disperse boundary. This velocity can be found from the following equation, which is similar to Eq. 50:

$$\mu_2 = D\{c_2(\mu_2), 0\} \tag{57}$$

Then, for the right edge of the front disperse boundary, we find

$$\bar{x}_r(t) = \mu_2 t + x_0 \tag{58}$$

It is important to note that, since μ_2 satisfies Eq. 57 and at the same time is the concentration velocity, the velocity μ_2 is the velocity $v(c_*)$

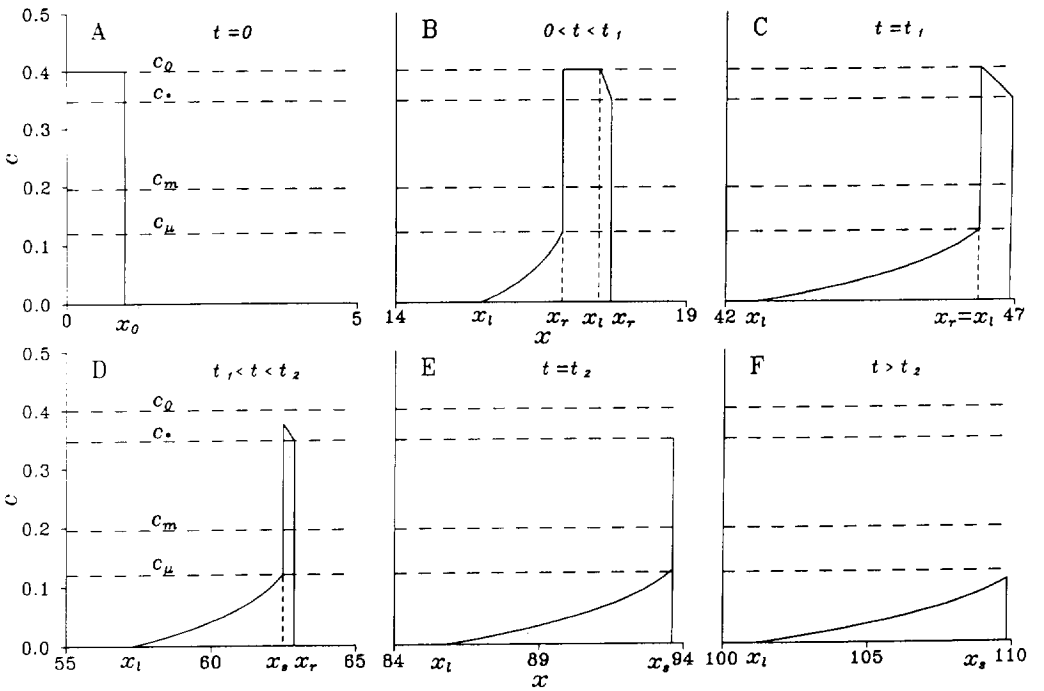

Fig. 11. Structure of the peaks shown in Fig. 10. Peaks A–C are plotted on the same scale (on the x-axis), which is, however, different from the scale used for peaks D–F. (A) Initial "rectangular pulse" distribution at $t = 0$, $x_0 = 1$. (B) A peak with a disperse rear boundary, right discontinuity, a region of constant initial concentration, a front disperse boundary and a front discontinuity, $t = 20.1$. (C) A peak at the time moment $t = t_1 = 55.3$ when the rear disperse boundary reaches the front disperse boundary. (D) A peak with a rear disperse boundary, a discontinuity, a front disperse boundary and a front discontinuity. The concentration at the peak maximum decreasing as the peak moves along the capillary, $t = 74.5$. (E) The second peak transformation: the right edge of the rear disperse boundary reaches the right edge of the front disperse boundary, $t = t_2 = 111.5$. (F) The final stage of the peak evolution, $t = 131.5$.

corresponding to the intercept of the concentration velocity and the discontinuity velocity curves. Therefore, the concentration corresponding to the amplitude of the front discontinuity is $c_{\mu_2} = c_*$, given by Eq. 29 and illustrated in Fig. 4.

At a time t_1 the right edge of the rear disperse boundary x_r reaches the left edge of the front disperse boundary $\bar{x}_l$ (Figs. 10C and 11C). The time t_1 is found from the following equation:

$$t_1 = \frac{x_0}{\mu_1 - v(c_0)} \tag{59}$$

The motion of the new right edge of the rear disperse boundary is found from the following equation:

$$\frac{d\bar{x}_s}{dt} = D_{c_1,c_2} \equiv D\left\{c_1\left(\frac{\bar{x}_s}{t}\right), c_2\left(\frac{\bar{x}_s - x_0}{t}\right)\right\} \tag{60}$$

with the initial condition

$$\bar{x}_s(t_1) = \frac{\mu_1 x_0}{\mu_1 - v(c_0)} \tag{61}$$

The problem in Eqs. 60 and 61 can be solved numerically.

The next transformation of the peak occurs when the boundary $\bar{x}_s$ reaches the right edge of the front disperse boundary $\bar{x}_r$ (Figs. 10C and 11C). The time moment t_2 when this event occurs is calculated from

$$\bar{x}_s(t_2) = \bar{x}_r(t_2) \tag{62}$$

After that the peak becomes "triangle"-like and

its further evolution is described again by Eqs. 41 and 43.

It is interesting that the time t_2 of the second transformation after which the peak becomes "triangle"-like is longer than in previous cases of lower initial concentration. This makes it possible to observe experimentally all stages of the peak evolution. The analysis presented above fully settles the case of the non-monotonous dependence of the concentration velocity on concentration. This type of velocity dependence on concentration reflects the fact that the electromigration and chromatographic mechanisms of the peak dispersion are comparable and act in opposite directions. We have seen in Fig. 1 (1.1) that electromigration in the case of $\alpha > 0$, corresponding to a decreasing dependence of the concentration velocity on concentration, leads to the development of a peak with a front disperse boundary. Chromatography, characterized by an increasing concentration dependence of the concentration velocity, in contrast, produces peaks with a rear disperse boundary. Combination of both, as shown above, is able to delay peak transformation significantly and thus preserve a narrow peak of the analyte.

We proceed to the following two cases of the concentration velocity monotonously increasing with concentration [case (ii), Eq. 22] and of the concentration velocity monotonously decreasing with concentration [case (iii), Eq. 23]. The analysis of the peak transformations is similar to that presented above, although there are qualitative differences in the peak behaviour.

5.2. Case (ii) Peak evolution with monotonously increasing velocity $\alpha < 0$, $(1 + \alpha c) > 0$

The initial concentration cannot be arbitrary high, otherwise the electric conductivity will become negative for high values of concentration. It is assumed below that the concentration is limited by the inequality $c < -1/\alpha$. The evolution of a concentration profile is shown in Fig. 12 (12.1).

The initial pulse (A) transforms into the peak (B) with a disperse rear boundary and a front discontinuity. The disperse boundary reaches the discontinuity (C) and the peak becomes "triangle"-like (D). The motion of the edges x_l, x_r and boundaries x_s, $\bar{x}_s$ is given by Eqs. 33–37. The asymptotic Eqs. 39–45 are also valid. A qualitative difference of the peaks shown in Fig. 12 (12.1) from those shown in Figs. 1 (1.1) and 5 is in the shape of the disperse boundary. In contrast to the peaks in Figs. 1 (1.1) and 5, the concentration profiles B, C, D in Fig. 12 (12.1) have an inflection point. In practice, a concentration profile with an inflection point might be misinterpreted as a diffusional boundary.

5.3. Case (iii). Peak evolution with monotonously decreasing velocity $\alpha > 0$, $k_1(k_2 - \alpha) < \alpha$

The peak evolution for this case is illustrated in Fig. 12 (12.2). It passes the following stages. The initial "rectangular pulse" (A) keeps a discontinuity at the rear and develops a disperse boundary at the front (B). The coordinates of the discontinuity and the edges of the disperse boundary are given by

$$x_s(t) = D_{c_0,0}t\,, \quad x_l(t) = v(c_0)t + x_0\,,$$
$$x_r(t) = v(0)t + x_0 \tag{63}$$

At the time moment t_1,

$$t_1 = \frac{x_0}{D_{c_0,0} - v(c_0)} \tag{64}$$

the discontinuity reaches the left edge of the disperse boundary (C) and after that the amplitude of the peak decreases and generates again the "triangle"-like shape (D). The coordinates of the discontinuity and the maximum concentration are found from a numerical solution of the equation

$$\frac{d\bar{x}_s}{dt} = D\left\{0, c_1\left(\frac{\bar{x}_s - x_0}{t}\right)\right\} \tag{65}$$

with the initial condition

$$\bar{x}_s(t_1) = x_0 \cdot \frac{D_{0,c_0}}{D_{c_0,0} - v(c_0)} \tag{66}$$

The asymptotic solution for the peak is also found analogously to Eqs. 39–45. However, the sign of the constant b in Eq. 43 is negative:

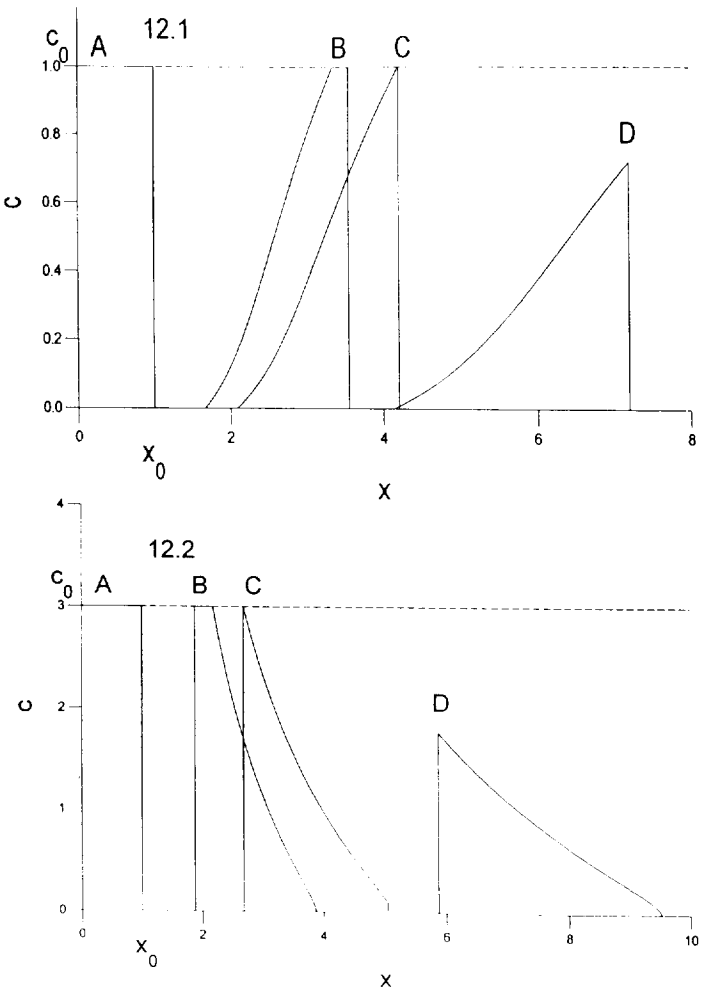

Fig. 12. (12.1) Peak evolution in the case of monotonously increasing concentration velocity. $\alpha = -0.2$, $k_1 = 0.3$, $k_2 = 4$, $c_0 = 1$. $v(0) = 0.7692$, $v(c_0) = 1.544$, $D_{c_0,0} = 1.179$. (A) Initial distribution $t = 0$, $x_0 = 1$. (B) A peak with a disperse rear boundary, a region of constant initial concentration and a discontinuity at the front. (C) The moment of the peak transformation into a "triangle", $t_1 = 2.74$. (D) The final stage of the peak evolution. (12.2) Peak evolution in the case of monotonously decreasing concentration velocity. $\alpha = 0.2$, $k_1 = 0.05$, $k_2 = 4$, $c_0 = 3$. $v(0) = 0.952$, $v(c_0) = 0.391$, $D_{c_0,0} = 0.6223$. (A) Initial distribution, $t = 0$, $x_0 = 1$. (B) A peak with a discontinuity at the rear, a region of constant initial concentration and disperse front. (C) The moment of the peak transformation into a "triangle", $t_1 = 4.3$. (D) The final stage of the peak evolution.

$$b = -\sqrt{-\frac{2\psi(c_0)v'(0)x_0}{1+k_1}} \tag{67}$$

6. Conclusions

In chromatography and electrophoresis, the concentration velocity is a monotonously increasing (non-linear chromatography and electrophoresis $\alpha < 0$) or a monotonously decreasing (electrophoresis $\alpha > 0$) function of the concentration. This leads to relatively simple and fast transformations of the initial "rectangular pulse" to a "triangle"-like peak. Combination of electrophoresis and non-linear adsorption can lead to a non-monotonous dependence of the concentration velocity on concentration and, as a result, to variety of peak shapes and scenarios of peak evolution.

The mechanisms of electromigration peak dis-

persion and non-linear chromatographic peak broadening are shown to be able partially to counterbalance each other. This is expressed in the long time required for transformation of the initial distribution into a "triangle"-like peak.

One of the most interesting findings, from a practical point of view, presented in this paper is that, depending on the initial concentration of an analyte, one may observe a peak as a "triangle"-like peak or as a peak with sharp discontinuities at its front and/or rear.

Variations of the capillary length, applied voltage or amount of the injected analyte may also lead to the appearance of all the kinds of peaks shown in this paper.

Acknowledgements

This work was supported in part by a grant from the European Community, Biomed I (No. Gene-93-0018) and by the Comitati di Biologia e Medicina e Chimica (CNR, Rome) to P.G.R.

References

[1] J.N. Jorgenson and K.D. Lukacs, *Science*, 222 (1983) 266–272.
[2] S. Hjértén, *Chromatogr. Rev.*, 9 (1967) 122–219.
[3] R. Virtanen, *Acta Polytech. Scand.*, 123 (1974) 1–67.
[4] S. Hjértén, *Electrophoresis*, 11 (1991) 665–690.
[5] F.M. Everaerts, T.A. van de Goor, Th.P.E.M. Verheggen and J.L. Beckers, *J. High Resolut. Chromatogr.*, 12 (1989) 28–31.
[6] S.F.Y. Li, *Capillary Electrophoresis—Principles, Practice and Applications*, Elsevier, Amsterdam, 1992, pp. 155–198.
[7] F.G. Helffrich, *J. Chromatogr.*, 629 (1993) 95–96.
[8] F.G. Helffrich and P.W. Carr, *J. Chromatogr.*, 629 (1993) 97–122.
[9] G. Klein, *AIChE Symp. Ser.*, 81, No. 242 (1985) 28.
[10] F.E.P. Mikkers, F.M. Everaerts and Th.P.E.M. Verheggen, *J. Chromatogr.*, 169 (1979) 1–10.
[11] V.G. Babskii, M.Yu. Zhukov and V.I. Yudovich, *Mathematical Theory of Electrophoresis*, Consultants Bureau, New York, 1989.
[12] R.A. Mosher, D.A. Saville and W. Thormann, *The Dynamics of Electrophoresis*, VCH, Weinheim, 1992.
[13] V. Sustacek, F. Foret and P. Boček, *J. Chromatogr.*, 545 (1991) 239–248.
[14] P.D. Lax, *Commun. Pure Appl. Math.*, 10 (1957) 537–566.
[15] G.B. Withem, *Linear and Non-Linear Waves*, Wiley, New York, 1974.
[16] B.L. Rozdestvenskii and N.N. Yanenko, *The Systems of Quasilinear Equation*, Nauka, Moscow, 1978 (in Russian).
[17] J.L. Wade, A.L. Bergold and P.W. Carr, *Anal. Chem.*, 59 (1987) 1286–1295.
[18] S. Golshan-Shirazi and G. Guiochon, in F. Dondi and G. Guiochon (Editors), *Theoretical Advancement in Chromatography and Related Separation Techniques*, Kluwer, Dordrecht, 1992, pp. 1–33.
[19] T. Tsuda, *Anal. Chem.*, 59 (1987) 521–523.
[20] W.D. Pfeffer and E.S. Yeung, *J. Chromatogr.*, 557 (1991) 125–136.